6

Quasicrystalline Materials

Zbigniew M. Stadnik

1. INTRODUCTION

The discovery of an icosahedral Al-Mn alloy by Shechtman et al.[1] extended the dichotomous division of solids into either crystalline or amorphous by introducing the notion of quasiperiodic crystals, or quasicrystals. This new form of matter possesses long-range *quasiperiodic* order and long-range orientational order associated with the classically forbidden fivefold (icosahedral), eightfold (octagonal), tenfold (decagonal), and twelvefold (dodecagonal) symmetry axes.[2-4] A central problem in condensed matter physics is to determine whether quasiperiodicity leads to physical properties which are significantly different from those of crystalline and amorphous materials. The majority of known quasicrystals are either icosahedral (*i*-) or decagonal (*d*-) alloys. A few known octagonal and dodecagonal alloys cannot be produced in sufficient quantities to allow studies of their physical properties.

The first few years of studies of quasicrystals revealed that their physical properties are similar to either their corresponding crystalline or amorphous (*a*-) counterparts.[5] For example, the values of the electrical resistivity, ρ, and its temperature dependence for *i*-$Al_{86}Cr_8Fe_6$ are very similar to those for an amorphous alloy $Al_{87}Ce_{6.3}Fe_{6.7}$, see Fig. 1. It was only later realized that the first quasicrystals, which were thermodynamically *metastable*, possessed significant structural disorder, as manifested in the broadening of the x-ray- and/or electron-diffraction lines. They also contained non-negligible amounts of second phases. The poor quality of these samples hampered the detection of those properties which could be intrinsic to quasiperiodicity. They also led to confusion, especially in the area of the magnetic properties of quasicrystals, where some "unusual" magnetic properties were claimed to have been observed.[8] Some of these properties were later shown[9,10] to result from the presence of magnetic second phases in the icosahedral alloys studied. Therefore the discovery at the end of the 1980's of thermodynamically *stable* quasicrystals was of great importance because these stable, single-phase quasicrystals possess a high degree of structural perfection[11] comparable

Zbigniew M. Stadnik • Department of Physics, University of Ottawa, Ottawa, Ontario K1N 6N5, Canada

Mössbauer Spectroscopy Applied to Magnetism and Materials Science, Volume 2, edited by Gary J. Long and Fernande Grandjean. Plenum Press, New York, 1996.

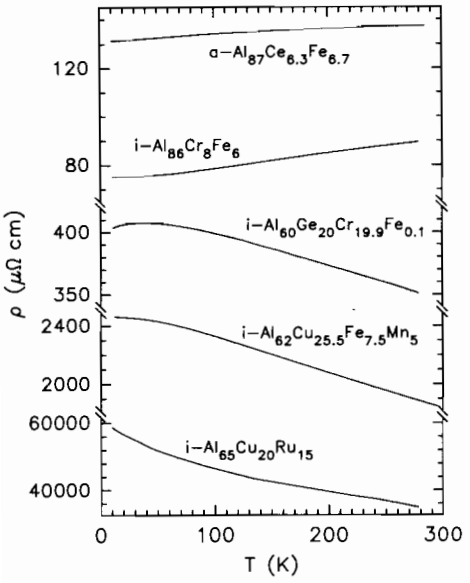

Figure 1. The temperature dependence of the electrical resistivity of some icosahedral and amorphous alloys.[6,7]

to that found in the best periodic alloys.

This chapter will provide an up-to-date review of some of the most unusual properties of quasicrystals and the role Mössbauer spectroscopy played in elucidating a better understanding of these complex and fascinating alloys.

2. STRUCTURAL MODELS OF QUASICRYSTALS

In spite of an enormous theoretical and experimental effort, the atomic structure of quasicrystals is still unknown, although some fundamental structural principles are now understood.[2-4,12] There are three principal models of the atomic structure of quasicrystals. The perfect quasicrystal model is based upon the concept of the Penrose tiling. Within this model, an icosahedral lattice, for example, is described in terms of a three-dimensional cut through a six-dimensional periodic lattice. Thus a high dimensional crystallography has to be employed to derive structural information from the diffraction data. The second model, the so-called random-tiling model, introduces some randomness into the quasilattice by replacing the strict matching rules in the ideal quasicrystal model with weaker ones. And finally, the glass model is based upon a random packing of icosahedral clusters. A more detail description of these models is beyond the scope of this chapter and therefore a reader should consult the literature.[2-4,12]

Quasicrystals, just as amorphous alloys, lack long-range periodic order. Therefore, diffraction methods upon which the bulk of our knowledge on the structure of quasicrystals is based, must be supplemented by local probes, such as Mössbauer spectroscopy, extended x-ray-absorption fine structure, nuclear quadrupole resonance, or nuclear magnetic resonance, if

the true atomic structure of quasicrystals is to be understood. This is because some theoretical structural models may produce diffraction patterns which are indistinguishable within the finite experimental resolution, whereas they may produce different sets of hyperfine parameters and thus can be unambiguously differentiated by the local probes. The contribution of Mössbauer spectroscopy to the structural studies of quasicrystals is discussed in Section 4.

3. UNUSUAL PROPERTIES OF QUASICRYSTALS

3. 1. Brief Survey of Properties of Quasicrystals

The new stable icosahedral alloys with a high degree of structural perfection exhibit some unexpected behavior. First, their most salient feature, which is not expected for alloys formed of normal metallic elements, is the very high value of ρ, or the very low value of the electrical conductivity, σ.[13-17] These ρ or σ values are several orders of magnitude larger or smaller than those of the constituent metals or of the amorphous alloys, and are comparable to those of doped semiconductors. This is illustrated in Fig. 1, where the ρ values in *i*-$Al_{62}Cu_{25.5}Fe_{7.5}Mn_5$ and *i*-$Al_{65}Cu_{20}Ru_{15}$ are respectively an order and two orders of magnitude larger than those in *i*-$Al_{86}Cr_8Fe_6$ and *a*-$Al_{87}Ce_{6.3}Fe_{6.7}$. Such high ρ values correspond to σ values which are comparable to or smaller than the Mott's "minimum metallic conductivity" of 200 $\Omega^{-1}cm^{-1}$ for the metal-insulator transition.[18] It was even suggested[17] that *i*-Al-Pd-Re alloys are insulators at low temperatures. Second, the temperature coefficient of ρ of these new icosahedral alloys is generally negative, which is inconsistent with the expected behavior for metals. A very small increase of ρ with decreasing temperature is also observed for some metastable icosahedral alloys, such as *i*-$Al_{60}Ge_{20}Cr_{19.9}Fe_{0.1}$, see Fig. 1. Third, the ρ values are extremely sensitive to the sample composition,[16,17,19] which is reminiscent of doping effects in semiconductors. Fourth, the ρ values of these stable icosahedral alloys increase as their structural quality improves as occcurs upon annealing which removes the defects,[5,17] in contrast to the behavior of typical metals. Other unexpected anomalies in the transport properties of icosahedral alloys involve a very low electronic contribution to the specific heat, large and strongly temperature-dependent Hall coefficients and thermoelectric power, and a non-Drude-like optical conductivity.[11] From a magnetic point of view, the stable icosahedral alloys of high structural quality are unusual in that they are diamagnetic[20,21] in spite of containing a significant concentration of transition-metal atoms.

Quasicrystals of decagonal symmetry combine two structural characteristics; they are quasiperiodic with tenfold symmetry in planes which are stacked with translational periodicity along the tenfold axis perpendicular to them. As expected, their physical properties are anisotropic. For example, ρ has metallic characteristics along the periodic direction and exhibits a nonmetallic behavior, similar to that observed in icosahedral alloys, in the quasiperiodic plane.[22]

3. 2. Models of the Electronic Structure of Quasicrystals

A fundamental question in the physics of quasicrystals is the origin of the unusually low values of σ. The first suggested interpretation, which still prevails, is based upon a Hume-Rothery mechanism,[3-5,11,13] which implies the existence of a pseudogap in the electronic density of states in the vicinity of the Fermi level, E_F. Initially, the Hume-Rothery mechanism was invoked, both from the structural[23] and theoretical[24] side, in relation to the problem of the stability of quasicrystals. It was later linked[25] to the small σ values through the Einstein

equation,[18] $\sigma = e^2DN(E_F)$, in which D is the electron diffusion coefficient, i.e., the diffusivity, and $N(E_F)$ designates the density of states at E_F. The correlation between the low σ and the low $N(E_F)$ was based upon the experimental observation of the very small value of the electronic contribution to the specific heat, γ,[5,25] which is directly proportional to $N(E_F)$. Support for the Hume-Rothery mechanism in icosahedral alloys also comes from the results of the NMR[26] and optical conductivity[27] experiments which were interpreted in terms of low $N(E_F)$ or the existence of a pseudogap in the density of states around E_F. The reduced $N(E_F)$ is also consistent with the observed diamagnetism.[20,21] Furthermore, the notion of a structure-induced pseudogap in the density of states around E_F results not only from theory based on the nearly-free-electron approximation[24,28] but is also supported by the electronic structure calculations for the lowest-order crystalline approximants of icosahedral alloys,[29-31] including the approximants containing transition metals atoms.[30,31] Approximants are complex crystalline phases close in composition to quasicrystals and with known structures; their local atomic configurations are close to those expected in the corresponding quasicrystals. Apart from its seeming simplicity, expressed in the relation $Q = 2k_F$,[23] where Q is the magnitude of the reciprocal lattice vector corresponding to the strongest x-ray reflection and k_F is the radius of the Fermi sphere, the Hume-Rothery mechanism is so appealing because it can explain qualitatively why the stable icosahedral alloys have both the lowest values of σ and γ. It can also be used to rationalize qualitatively why stable icosahedral alloys exist only in a rather narrow composition range and why a small composition change can shift the E_F away from the density of states minimum.

The experimental studies mentioned above provide *indirect* information on the density of states at one particular energy, E_F. To determine the electronic structure of quasicrystals, and in particular the possible existence of a pseudogap in the density of states around E_F, spectroscopic techniques which probe density of states *directly*[11,22] must be used. Unfortunately, due to insufficient energy resolution available, these spectroscopic experiments could not unambiguously verify whether the minimum in the density of states around E_F does exist.

Some of the recent low-temperature, high energy-resolution ultraviolet photoemission spectroscopy results[32,33] obtained at a photon energies of 21.2 eV, from He I, and 40.8 eV, from He II, are presented here. They convincingly solve the problem of the minimum of the density of states at E_F.

Figure 2a shows a theoretical He II valence band predicted for an *i*-Al-Cu-Fe alloy.[32] The theoretical calculations[30] of the density of states were performed for a 1/1 approximant of an *i*-Al-Cu-Fe alloy. A clear depression of intensity, which is proportional to the total density of states, towards E_F is clearly seen, with the predicted density of states minimum being slightly above E_F. Additionally, the theory[29-31] predicts the presence of many narrow spikes in the density of states, see Fig. 2a. This spikiness is believed to be a specific property which distinguishes quasicrystals from amorphous and crystalline alloys. However, the predicted pseudogap is not such a property because it is also present in some amorphous and crystalline alloys. To make a meaningful comparison of the theoretical band in Fig. 2a with the measured one, the former has to be multiplied by the Fermi-Dirac distribution function corresponding to the temperature of an experiment, and appropriately broadened to account for the lifetime broadening effects inherent to the ultraviolet photoemission spectroscopy technique and for the finite instrumental resolution.[11,22] Such a broadened band in the vicinity of E_F is shown in Fig. 2b.

Figure 3a shows the valence band of a well-characterized single-phase *i*-$Al_{65}Cu_{20}Fe_{15}$. Two broad features at the binding energies of about -1 and -4 eV are due respectively to states of the iron 3d and Cu 3d character,[34] in good agreement with the theoretical predictions, see

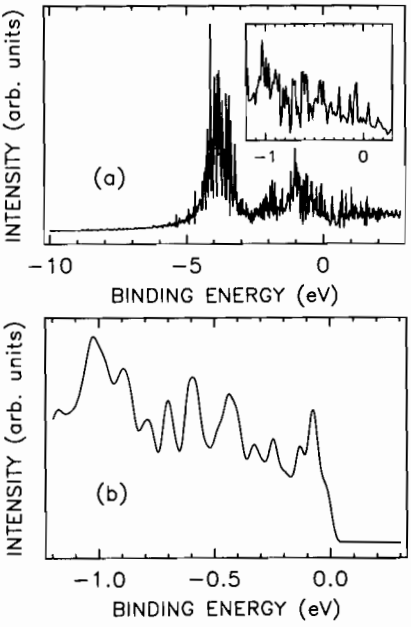

Figure 2. (a) The theoretical 40.8 eV ultraviolet photoemission spectroscopy valence band of the 1/1 approximant of an *i*-Al-Cu-Fe alloy obtained by summing the theoretical partial aluminum, copper, and iron density of states associated with different angular momenta, from ref. 30, weighted by the corresponding photoionization cross sections and by the composition and the number of electrons, as described in reference 22. The inset shows a part of the band around E_F. The binding energy is referred to E_F. (b) Part of the theoretical band close to E_F from (a) which was multiplied by the Fermi-Dirac distribution function at 14 K and convoluted with a Lorentzian, $\Gamma_L^0 = 0.02$ eV^{-1}, to account for the lifetime broadening, see ref. 22, and with a Gaussian with full width at half maximum of 31 meV, to account for the instrumental broadening.

Fig. 2a and reference 30. A sharp intensity decrease towards E_F and an indication of the presence of a Fermi edge can also be noticed, see Fig. 3a. These two characteristics are clearly seen in the valence band measured in the vicinity of E_F, Fig. 3b. Three observations are apparent from Fig. 3b. First, there is a strong intensity decrease towards E_F, which can be interpreted as being due to the presence of a pseudogap centered in the vicinity of E_F. A more quantitative interpretation of this observation is given below. Second, a clear Fermi edge is observed, which constitutes the spectroscopic proof that the system is metallic. A similar earlier study[35] of *i*-$Al_{65}Cu_{21}Fe_{14}$ carried out at room temperature and with the resolution of 233 meV concluded that there is no well-defined Fermi edge in the *i*-Al-Cu-Fe alloy. Third, there is no evidence for the existence of spikes which should be observed clearly for the energy resolution used in the experiment, see Fig. 2b.

One can reproduce the observed structure of the valence band close to E_F, see Fig. 3b, by using a simple model suggested in reference 35. It can be noticed in Fig. 3b that the intensity increases towards E_F for binding energies between -1.2 and about -0.9 eV. The model[35] thus assumes that without a pseudogap, the density of states at 0 K, which can be called the normal density of states, would increase linearly up to E_F, see Fig. 4a. It is then assumed[35] that the normal density of states has a dip in a Lorentzian shape centered at E_F, with the half-width, G_L, and the dip depth, C, relative to the normal density of states. One can obtain a relatively good fit, as shown by the solid line in Fig. 4b, for $G_L = 0.36(1)$ eV and $C = 0.70(1)$. It can be thus concluded that, in agreement with an earlier analysis,[35] the observed intensity depression close to E_F in the valence band of *i*-$Al_{65}Cu_{20}Fe_{15}$ can be accounted for by a pseudogap of the

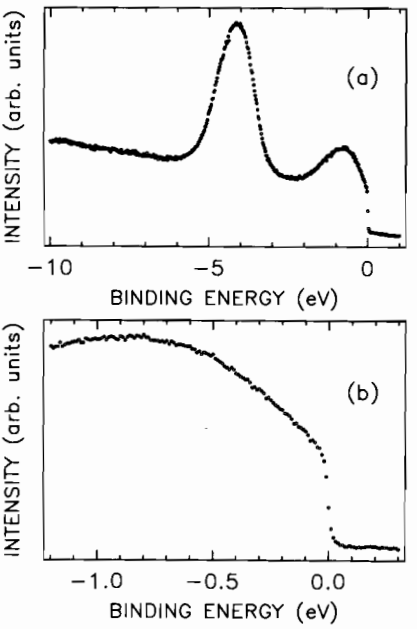

Figure 3 (a). The valence band of i-$Al_{65}Cu_{20}Fe_{15}$ measured at 40.8 eV and 14 K with the energy resolution of 42 meV, see reference 32. The data were not corrected for the background due to the inelastic electron scattering. (b) The valence band of i-$Al_{65}Cu_{20}Fe_{15}$ in the vicinity of E_F measured at 40.8 eV and 14 K with the energy resolution of 31 meV, see reference 32.

half-width of 0.36(1) eV and that the density of states at E_F is reduced by 70(1) percent with respect to the normal density of states at E_F.

The predicted spikiness could not be observed even with an energy resolution of 7.5 meV, see Fig. 5. Such a resolution represents the ultimate experimental conditions now achievable in a photoemission spectroscopy measurement of solids.[36] The temperature evolution of the leading edge of the valence band of i-$Al_{65}Cu_{20}Fe_{15}$ follows the temperature evolution of the Fermi-Dirac distribution function, see Fig. 5b, which additionally confirms the metallic character of the i-$Al_{65}Cu_{20}Fe_{15}$ alloy.

Valence bands similar to those shown in Figs. 3 and 5 were also obtained[32] for other stable icosahedral and dodecagonal alloys, except for the i-Al-Pd-Re system[33] in which no well-defined Fermi edge was observed, as is shown in Fig. 6, which also shows that there is a very low intensity at E_F in this system. This proves that the i-Al-Pd-Re system is nonmetallic.

In conclusion, the ultra-high-resolution ultraviolet photoemission spectroscopy experiments[32,33] provide a direct experimental proof that there is a wide pseudogap in the vicinity of E_F which must be partially responsible for the observed high values of ρ. All known quasicrystals, except for the i-Al-Pd-Re system, are metallic as evidenced by a clearly developed Fermi edge. The lack of the Fermi edge in the i-Al-Pd-Re system is consistent with its insulator behavior at low temperatures.[17] The possible reasons for the absence of the predicted spikiness of the density of states are discussed in Section 5.

There are experimental arguments which indicate that the Hume-Rothery mechanism alone is insufficient to explain the high values of ρ or the low values of σ. The dramatic changes of σ, of up to two orders of magnitude, with composition[13,15-17,19,37,38] and structural

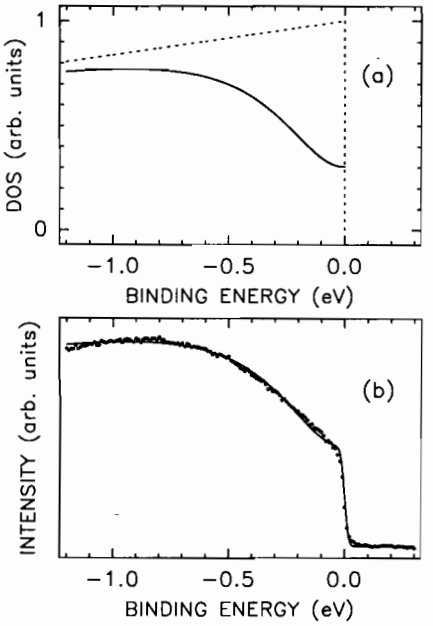

Figure 4. (a) The model[35] of density of states at 0 K which is used to fit the valence band in Fig. 3b. The broken line, which was obtained from a linear fit of the band in Fig. 3b between the binding energies -1.2 and -0.9 eV, represents the normal density of states, without the presence of a pseudogap. The solid line designates the dip which must be subtracted from the normal density of states in order to fit the band in Fig. 3b. (b) The valence band from Fig. 3b, circles, fitted, solid line, to the model density of states shown in (a).

quality[5,13,17,39] have been observed for *i*-samples whose values of γ differ only by up to about 10 percent. For example, the values of σ at 2 K and γ for *i*-$Al_{69}Pd_{19}Re_{12}$ are respectively 1000 $\Omega^{-1}cm^{-1}$ and 0.28 mJ/mol.K^2, see reference 38. The corresponding values for *i*-$Al_{67}Pd_{23}Re_{10}$ are 100 $\Omega^{-1}cm^{-1}$ and 0.25 mJ/mol.K^2, see reference 38. As both σ in the Einstein equation and γ are proportional to $N(E_F)$, the above experimental fact indicates that the small values of σ cannot be associated only with the minimum in the density of states at E_F. This is supported by the observation of the lack of the expected correlation between σ and the electron per atom ratio, e/a, in the *i*-Al-Cu-Fe system.[39] No correlation was also observed between the Hall coefficient and e/a in this system.[39] Additionally, the Einstein equation assumes that σ is proportional to the electron scattering time, which implies that σ should increase by removing the defects. The opposite is observed for icosahedral alloys.[5,16,17,19,40,41] This proportionality also predicts that σ should decrease with increasing temperature, which is contrary to the observed steep increase of σ with temperature at temperatures well above the Debye temperature.[13,17,19] Since σ in the Einstein equation is proportional to the product $DN(E_F)$, the unusually small values of σ may also originate from the reduced D.

The arguments presented above suggest that a simple interpretation based on the Einstein equation is not applicable to icosahedral alloys and alternative approaches are required to explain the unusual properties of these alloys. These new approaches are based on the concepts of tunnelling, localization, and critical states. One of the first of such approaches, which is very qualitative and which claims to give a good explanation of the electronic properties of icosahedral alloys, is based on an internal structural model.[42] It assumes the presence of the conductive icosahedral blocks which are enveloped by an insulating layered-

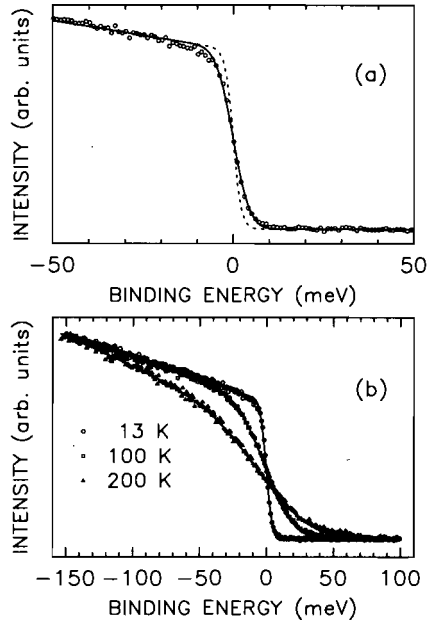

Figure 5. (a) The near-E_F spectrum of i-$Al_{65}Cu_{20}Fe_{15}$ measured at 21.2 eV and 13 K. The solid line is the fit to a linearly decreasing intensity multiplied by the Fermi-Dirac distribution function at 13 K, the broken curve, and convoluted with a Gaussian whose linewidth is 7.5 meV. Note that the step between the data points is 1 meV, see reference 32. (b) The temperature-dependent ultraviolet photoemission spectra of i-$Al_{65}Cu_{20}Fe_{15}$ near E_F measured at 21 eV. The solid lines are the fits to a linearly decreasing intensity multiplied by the Fermi-Dirac distribution function at the corresponding temperature and convoluted with a Gaussian whose linewidth is 7.5 meV, see reference 32.

structure network. For this structural model the electrical conduction should occur via tunnelling. Such tunnelling should lead to deviations from Ohm's law; however, the law was obeyed perfectly in the i-Al-Cu-Fe film for bias voltages varying by seven orders of magnitude.[43] Another approach invokes the concept of localization.[18] Inherent to this concept is the notion of disorder which causes the electrons to become localized, i.e., spatially confined to some region of an icosahedral alloy. Conduction then occurs via thermal activation between the localized states, or hopping. Consequently, the very small values of σ can occur for the finite values of the density of states at E_F. The use of the localization approach to explain the electronic transport properties of icosahedral alloys was suggested by Kimura et al.[44] and was later invoked and elaborated in the following works.[17,45] The third approach is based upon the idea of the new type of electronic states, the so-called critical states, which are intermediate between the extended electronic states in metals and the localized electronic states in insulators. Such states were shown theoretically to exist in one- and two-dimensional quasiperiodic systems.[46] Although it is not clear whether the critical states can occur in realistic three-dimensional quasiperiodic systems, they may have profound consequences on the electronic transport properties of quasicrystals.[13,47,48] It can be concluded that there is no generally accepted explanation of the unusual transport properties of quasicrystals.

A relevant question related to the unusual properties of quasicrystals discussed above is to what extent is the quasiperiodicity essential for their occurrence. The observations[13,26] of similar unusual transport behavior in crystalline approximants indicate that it is the local atomic order, rather than the quasiperiodicity, which determines the properties of quasicrystals.

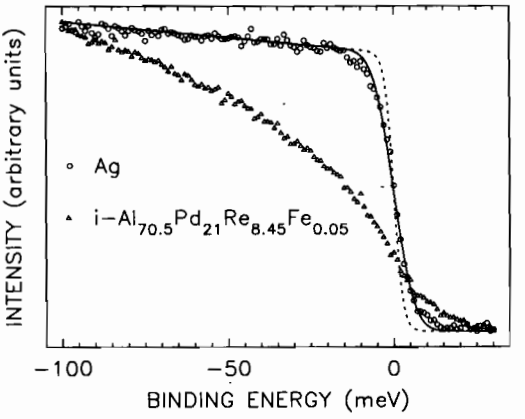

Figure 6. The near-E_F spectra of *i*-$Al_{70.5}Pd_{21}Re_{8.45}Fe_{0.05}$ and of silver evaporated onto *i*-$Al_{70.5}Pd_{21}Re_{8.45}Fe_{0.05}$ measured at 21.2 eV and 15 K, see reference 33. The resolution of the experiment was determined from the fit, solid line, of the silver spectrum to a linearly decreasing intensity multiplied by the Fermi-Dirac distribution function at 15 K, broken curve, and convoluted with a Gaussian whose linewidth was 10 meV.

4. HYPERFINE INTERACTIONS IN QUASICRYSTALS

Mössbauer spectroscopy is a local probe which can be used in studies of quasicrystals to obtain, in principle, two types of information. First, local atomic structure can be studied through the electric quadrupole interactions. The hyperfine parameters derived from the Mössbauer spectra must be compared with those calculated for a particular structural model if the full potential of Mössbauer spectroscopy is to be employed. Such calculations, however, are not trivial, especially for structurally complex quasicrystals. The first such calculations performed for a *d*-Al-Co-Cu alloy[50] will be compared below with the experimental Mössbauer data. Examples of Mössbauer spectra of representative quasicrystals and their analysis will be presented. Second, magnetic properties of quasicrystals can be investigated through the magnetic dipole interaction. Examples of such investigations will be discussed.

4. 1. Nonmagnetic Quasicrystals

Most quasicrystals are not magnetically ordered, but rather they are either paramagnetic or diamagnetic down to liquid helium temperatures.[20] Their Mössbauer spectra thus exhibit the combination of the electric monopole and quadrupole hyperfine interactions.[49] Mössbauer

spectra of most nonmagnetic quasicrystals consist of two very broad and structureless lines, with typical values for the full linewidth of the component lines in the range 0.35 to 0.45 mm/s, values which should be compared with the typical value of 0.23 mm/s for the full linewidth of the two inner lines of the Zeeman sextet of a thin α-iron calibration foil. However, as will be discussed below, Mössbauer quadrupole spectra of some quasicrystals exhibit clear structural features superimposed on the two broad lines, which can be, in principle, directly related to possible structural models. The presence of broad component lines shows that iron atoms are not in a single or in a few discrete local environments. The analysis of such Mössbauer spectra has to be then based on the distribution of the hyperfine interaction parameters.[49]

Mössbauer spectra of quasicrystals can be analyzed at two levels of sophistication. If only average values of the isomer shift, δ, and the quadrupole splitting, Δ, are of interest, then a simple fit with, for example, an asymmetric Lorentzian doublet is sufficient. The values of $\bar{\delta}$ and $\bar{\Delta}$ determined in this way have a relative error of less than a few percent. Increasing the number of fitted components, which may not have any physical justification, significantly improves the fit and the resulting $\bar{\delta}$ and $\bar{\Delta}$ values calculated from the fitted parameters of these components are determined more precisely. One gets a rather limited insight into the structural properties of quasicrystals only from the average values, $\bar{\delta}$ and $\bar{\Delta}$, because these values do not change significantly in metallic systems of different structures.

At another level of spectral analysis, one attempts to derive the distribution of quadrupole splittings, $P(\Delta)$, which is closest to the true one. It is the derived $P(\Delta)$ which is of great importance because it is directly related to the local atomic structure. However, deriving this distribution is not a simple task and there are many pitfalls which, if not avoided, lead to perfect fits with the $P(\Delta)$'s which are far from the true ones. A review of various methods of deriving $P(\Delta)$ and of various problems associated with this derivation is given in references 51 and 52 and in Chapter 5 of this book. There are generally two main approaches used to extract $P(\Delta)$. First, either a specific shape of $P(\Delta)$ is assumed, for example, a Gaussian shape or, second, no a priori assumption about the shape of $P(\Delta)$ is made, usually in conjunction with the constrained version[53] of the Hesse-Rübartsch method[54] or the Rancourt-Ping method.[52] The disadvantage of the first approach is that it presupposes the shape of $P(\Delta)$ which may differ considerably from the real $P(\Delta)$. The disadvantage of the Le Caër-Dubois version[53] of the second approach is the possibility of unphysical oscillations in $P(\Delta)$ for inappropriately chosen parameters which must be fixed in the fit. These oscillations do not occur in the Rancourt-Ping method.[52] Usually, a linear relation, $\delta = \delta_0 + \delta_1\Delta$, is assumed,[52,53] where δ_0 and δ_1 are the fitted parameters.

We used both the Le Caër-Dubois and Rancourt-Ping methods in the analysis of Mössbauer spectra of various quasicrystals.[55,56] The $P(\Delta)$'s, which are presented below, turned out to be essentially independent of the method used to extract them from the Mössbauer spectra.[55,56] This indicates that they are close to the true $P(\Delta)$'s. In many cases, the derived $P(\Delta)$ is of, or very close to, a Gaussian shape. One should note that the discussions[51-54] of various methods of deriving $P(\Delta)$ assume an ideal situation of a single-phase sample. In reality, most samples contain a few percent of a second phase/phases which may not be detected in a typical x-ray diffraction measurement. The presence of such a second phase can be detected[55] in Mössbauer spectra of many quasicrystals by carefully analyzing the residuals, i.e., the difference between the Mössbauer spectrum and the fit to a particular $P(\Delta)$. Accepting the presence of clear structural features in the residuals, and thus a value of χ^2 much larger than one, may distort[55] the derived $P(\Delta)$.

All Mössbauer absorbers used in our studies[55,56] were thin and homogeneous. They were prepared by mixing a pulverized alloy with a petroleum jelly, which resulted in a random

orientation of the sample particles. The low ratio of the absorber radius to the source-absorber distance assured that the cosine smearing effect was negligible. In all quasicrystals discussed below with the iron concentration smaller than 3 atomic percent, the iron metal used to prepare them was enriched to 95.9 percent in the iron-57 isotope. The velocity scale of all Mössbauer spectra presented here is relative to α-iron at room temperature.

4. 1. 1. Icosahedral Alloys

A typical Mössbauer spectrum of a metastable *i*-$Al_{60}Ge_{20}Cr_{19.9}Fe_{0.1}$, as is shown in Figure 7, can be fitted relatively well with a structureless Gaussian-like P(Δ), see Fig. 7c. A close inspection of the residuals in Fig. 7a indicates the presence of some structure due to an unaccounted impurity component. To a first approximation, this component can be taken in the form of a symmetric Lorentzian doublet. Its inclusion in the fit, as is shown in Fig. 7b, leads to a lowering of the χ^2 from 1.30 to 1.12 and to the disappearance of the residuals structure. Although for this particular icosahedral alloy the inclusion of the impurity doublet does not lead to a significant change of P(Δ), see Fig. 7c, it does for other quasicrystals.[55]

Both the Mössbauer spectra of metastable icosahedral alloys and the resulting P(Δ)'s, as illustrated in Fig. 7, are very similar to those characteristic for amorphous alloys.[58] It was thus initially thought that metastable icosahedral alloys are highly disordered and that Mössbauer spectroscopy will not be able to reveal any structural differences between these alloys and the corresponding amorphous counterparts. That this is not the case is illustrated in Fig. 8 in which the Mössbauer spectra and the resulting P(Δ)'s are compared for the $Al_{75}Cu_{14.85}Fe_{0.15}V_{10}$ alloy which can be produced both in an amorphous and icosahedral state.[59] The Mössbauer spectrum of *a*-$Al_{75}Cu_{14.85}Fe_{0.15}V_{10}$, see Fig. 8a, and the resulting P(Δ), Fig. 8(d), are very similar to those characteristic for the *i*-$Al_{60}Ge_{20}Cr_{19.9}Fe_{0.1}$ alloy, as is shown in Fig. 7. However, the Mössbauer spectra of *a*- and *i*-$Al_{75}Cu_{14.85}Fe_{0.15}V_{10}$ and the resulting P(Δ)'s, see Fig. 8, differ significantly, as may be noted by the presence of some structure at about -0.2 mm/s in the spectrum of *i*-$Al_{75}Cu_{14.85}Fe_{0.15}V_{10}$. An attempt to fit the spectrum of *i*-$Al_{75}Cu_{14.85}Fe_{0.15}V_{10}$ with one P(Δ) component and an impurity component, Fig.

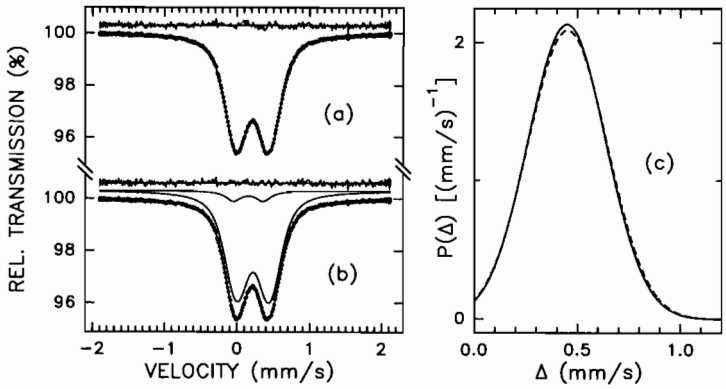

Figure 7. The room temperature Mössbauer spectrum of *i*-$Al_{60}Ge_{20}Cr_{19.9}Fe_{0.1}$ fitted with (a) one P(Δ) component, the solid line in (c), and with (b) the P(Δ), the broken line in (c) plus impurity components. The component spectra are also shown in (b). The residuals, multiplied by a factor of three, are shown above each spectrum.

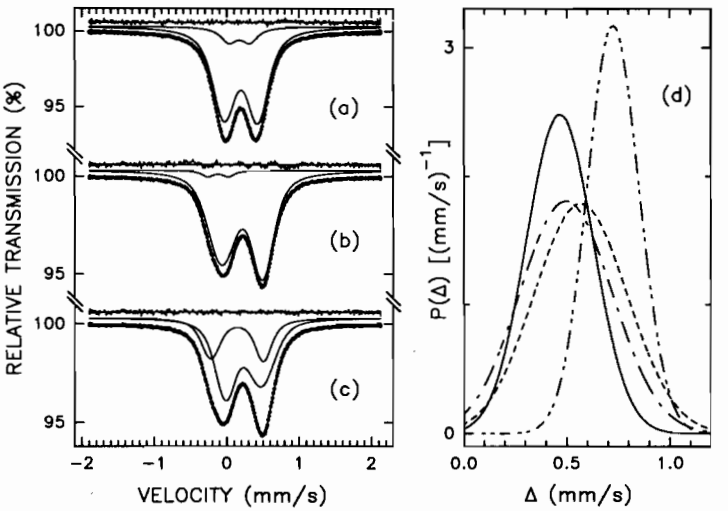

Figure 8. The room temperature Mössbauer spectra of (a) *a*-$Al_{75}Cu_{14.85}Fe_{0.15}V_{10}$ fitted with the P(Δ) and impurity components, and of *i*-$Al_{75}Cu_{14.85}Fe_{0.15}V_{10}$ fitted with the P(Δ) and impurity components (b), and with two P(Δ) components (c). The P(Δ)'s corresponding to fits in (a), the solid line, (b), the broken line, and (c), the dash-dot and dash-double-dot lines, are shown in (d). The residuals, multiplied by a factor of three, are shown above each spectrum.

8(b), does not produce the structureless residuals, $\chi^2 = 1.46$. Such residuals can be obtained only from a fit with two P(Δ)'s, see Fig. 8c, which results in $\chi^2 = 1.04$. These two P(Δ)'s are indicative that there must be two different classes of transition metal environments in *i*-$Al_{75}Cu_{14.85}Fe_{0.15}V_{10}$. Contrary to what one would expect, the $\bar{\Delta}$ value for *i*-$Al_{75}Cu_{14.85}Fe_{0.15}V_{10}$ is significantly larger than that for *a*-$Al_{75}Cu_{14.85}Fe_{0.15}V_{10}$, at 0.575(1) and 0.468(1) mm/s, respectively.

Another example showing the distinct differences in Mössbauer parameters corresponding to three different structures involves the Al-Cu-Fe system. For a particular composition in this system, one can produce samples in the amorphous, icosahedral, or cubic phases.[55,60] The $\bar{\Delta}$ values determined from the Mössbauer spectra[55] of the *a*-, *i*-, and *c*-$Al_{64}Cu_{24}Fe_{12}$, as are shown in Fig. 9, are respectively 0.535(1), 0.396(1), and 0.419(1) mm/s. The corresponding $\bar{\delta}$ values are 0.239(1), 0.230(1), and 0.247(2) mm/s. Note also that the P(Δ) of *i*-$Al_{64}Cu_{24}Fe_{12}$, which is a stable icosahedral alloy, is significantly narrower than that of metastable amorphous and cubic phases, see Fig. 9d, and than those P(Δ)'s of other metastable *i*-alloys, see Figs. 7c and 8d. This difference in width of P(Δ) can be related, at least partially, to the fact that the method by which they are produced results in the metastable samples containing various defects, reflected in broadening of the x-ray diffraction Bragg peaks,[55] whereas the stable *i*-$Al_{64}Cu_{24}Fe_{12}$ has no such defects, as is reflected in narrow Bragg

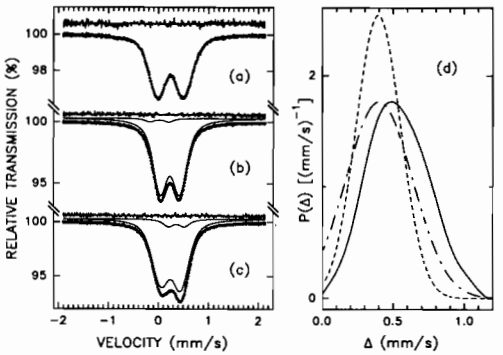

Figure 9. The room-temperature Mössbauer spectra of $Al_{64}Cu_{24}Fe_{12}$ in (a) the amorphous state fitted with one P(Δ), component, the solid line in (d), (b) the icosahedral state fitted with one P(Δ), the broken line in (d), and impurity components, and (c) the crystalline state fitted with one P(Δ), the dash-dot line in (d), and impurity components. The component spectra are also shown in (b) and (c). The residuals, multiplied by a factor of three, are shown above each spectrum.

peaks.[55] Nevertheless, the very fact that in the stable, structurally "perfect" *i*-$Al_{64}Cu_{24}Fe_{12}$ the P(Δ) has a finite and non-negligible width shows that there must be some type of structural and/or chemical disorder present even in the stable, structurally perfect *i*-alloys. The nature and role of this disorder will be discussed in Section 5.

Other stable *i*-alloys of high structural quality also exhibit the presence of P(Δ) in their Mössbauer spectra, as is shown in Fig. 10,[55,56] which supports the idea of the existence of some sort of topological and/or chemical disorder in these alloys. The values of the full width at half maximum of the P(Δ)'s corresponding to *i*-$Al_{64}Cu_{24}Fe_{12}$, Fig. 9, *i*-$Al_{65}Cu_{20}Fe_{7.5}Ru_{7.5}$, Fig. 10, and *i*-$Al_{70.5}Pd_{21}Re_{8.45}Fe_{0.05}$, Fig. 10, are 0.366(1), 0.451(1), and 0.358(2) mm/s, respectively. One notices that these values are very similar for the ternary stable alloys. The larger value for the quaternary *i*-$Al_{65}Cu_{20}Fe_{7.5}Ru_{7.5}$ alloy is mainly due to its increased chemical disorder. Also the $\bar{\Delta}$ values for these three *i*-alloys are quite similar, with values of 0.396(1), 0.410(1), and 0.404(2) mm/s, respectively. Furthermore, these alloys have a similar, Gaussian-like shape of P(Δ). These arguments suggest that the structure of *i*-Al-Cu-TM, where TM is Fe, Ru, and Os, see reference 55, and *i*-Al-Pd-Re, see reference 56, must be similar. Unfortunately, there are at present no theoretical calculations which would predict the P(Δ) for possible structural models of these alloys.

The Mössbauer spectra of *i*-alloys discussed above had essentially no structure, except for the spectrum of *i*-$Al_{75}Cu_{14.85}Fe_{0.15}V_{10}$ shown in Fig. 8, and consequently the corresponding P(Δ)'s had single-peaked, Gaussian-like shapes. Such a shape was also observed for other *i*-alloys.[61,62] Recent extensive studies[55] of various quasicrystals show that there are quasicrystalline systems with structured Mössbauer spectra, and therefore, with structured shapes of P(Δ)'s. This should be very helpful in placing stringent constraints on various structural models. A few examples of such Mössbauer spectra are presented below.

The Mössbauer spectrum of metastable *i*-$Al_{70}Pd_{20}Fe_{10}$ alloy[55,63] exhibits a very strong asymmetry, as is shown in Fig. 11. Its fit with one P(Δ) is clearly unsatisfactory as evidenced by the value of χ^2=1.30 and the structure present in the residuals. However, this fit already indicates that the shape of P(Δ) has a bimodal character, see Fig. 11c. The fit with one P(Δ) and an impurity component reduces χ^2 to 0.96, but the relative area under the impurity compo-

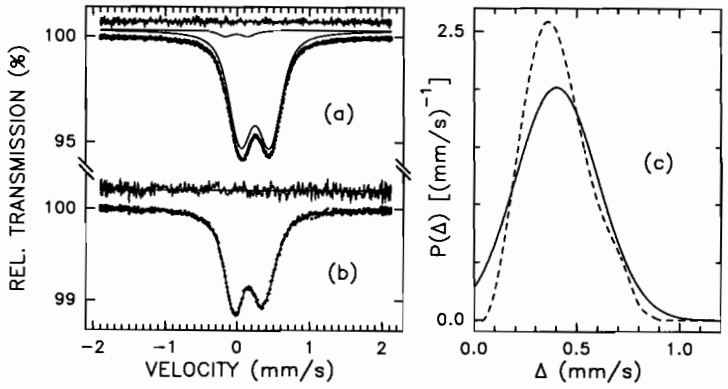

Figure 10. The room-temperature Mössbauer spectra of (a) i-$Al_{65}Cu_{20}Fe_{7.5}Ru_{7.5}$ fitted with one P(Δ) component, the solid line in (c), and impurity components and (b) i-$Al_{70.5}Pd_{21}Re_{8.45}Fe_{0.05}$ fitted with one P(Δ) component, the broken line in (c). The residuals, multiplied by a factor of three, are shown above each spectrum.

nent is 29 percent, which is much above the impurity concentration of a few percent expected from the x-ray diffraction spectrum.[55,63] An excellent fit with $\chi^2 = 0.93$ is obtained with two P(Δ) components, as is shown in Fig. 11b. It can be thus concluded there are two distinct classes of iron environments in this alloy, and any structural model has to take this fact into account.

The Mössbauer spectra[55] of stable i-$Al_{70}Pd_{20}Mn_{9.97}Fe_{0.03}$ and i-$Al_{70}Pd_{20}Cr_5Fe_5$ show distinct asymmetry and some structure. They cannot be fitted with one P(Δ), but satisfactory fits are obtained assuming the presence of two P(Δ)'s, see Fig. 12.

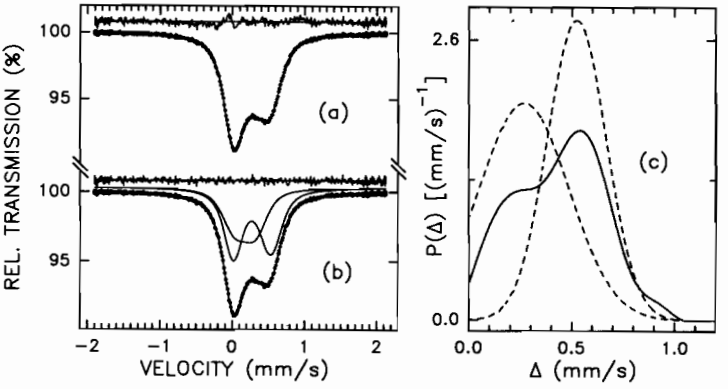

Figure 11. The room-temperature Mössbauer spectrum of i-$Al_{70}Pd_{20}Fe_{10}$ (a) fitted with one P(Δ) component, the solid line in (c) and (b) fitted with the two P(Δ) components, the broken lines in (c). The component spectra are also shown in (b). The residuals, multiplied by a factor of three, are shown above each spectrum.

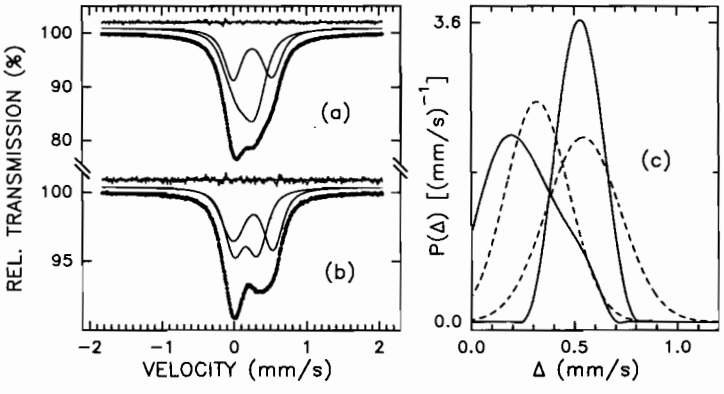

Figure 12. The room-temperature Mössbauer spectra (a) of *i*-$Al_{70}Pd_{20}Mn_{9.97}Fe_{0.03}$ fitted with two P(Δ) components, the solid lines in (c), and (b) of *i*-$Al_{70}Pd_{20}Cr_5Fe_5$ fitted with two P(Δ) components, the broken lines in (c). The component spectra are also shown. The residuals, multiplied by a factor of three, are shown above each spectrum.

4. 1. 2. Decagonal Alloys

Mössbauer spectra of decagonal alloys[55,64,65] generally possess more structure than those of *i*-alloys. For some *d*-systems a single-peaked, Gaussian-like P(Δ) is observed. This is illustrated in Fig. 13 for the stable[63,66] *d*-$Al_{75}Pd_{15}Fe_{10}$ alloy. As expected, a slightly narrower P(Δ) is obtained, see Fig. 13(c), for an annealed sample as compared to the P(Δ) of an as-cast sample.[66]

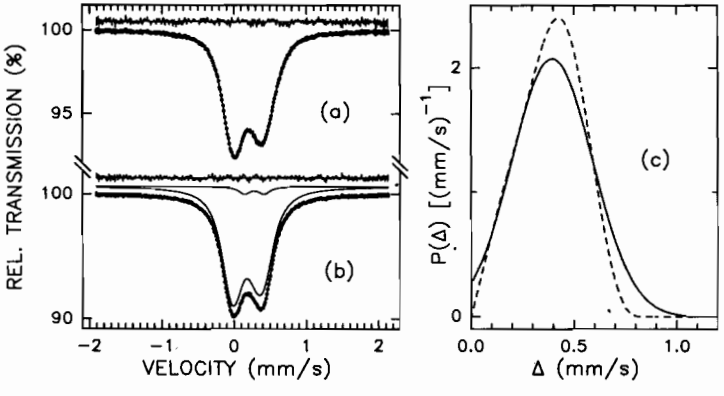

Figure 13. The room-temperature Mössbauer spectra of *d*-$Al_{75}Pd_{15}Fe_{10}$ (a) as cast and fitted with one P(Δ) component, the solid line in (c), and (b) after annealing, fitted with the P(Δ), the broken line in (c), and impurity components. The component spectra are also shown in (b). The residuals, multiplied by a factor of three, are shown above each spectrum.

The Mössbauer spectrum[55] of the metastable d-$Al_{70}Ni_{15}Fe_{15}$ alloy[67] cannot be fitted successfully with one P(Δ) component, as is clearly evidenced by the residual spectrum shown in Fig. 14a. Nevertheless, the derived P(Δ) is of a bimodal-type, see Fig. 14c, which indicates the possibility of two different classes of iron environments. An attempt to fit this spectrum with an additional impurity component[55] improves the fit, but the relative area of this component is 17 percent. This, however, is incompatible with the expected impurity concentration of a few percent from the x-ray diffraction pattern.[55] An excellent fit is obtained with two P(Δ) components, see Fig. 14b, which strongly suggests the existence of two structurally distinct classes of environments around the iron atoms in the d-$Al_{70}Ni_{15}Fe_{15}$ alloy.

The unquestionable evidence for the presence of at least two distinct classes of environments around transition metal atoms in some Al-transition metal d-alloys comes from the Mössbauer spectra of stable $Al_{70}Co_{15}Ni_{14.9}Fe_{0.1}$, see reference 65, and $Al_{65}Co_{15}Cu_{19.9}Fe_{0.1}$, see references 64 and 65, d-alloys. A visual inspection of the spectrum[55,65] of d-$Al_{70}Co_{15}Ni_{14.9}Fe_{0.1}$, see Fig. 15a, shows its clear asymmetry and the structure of the left absorption line. It is thus obvious that one needs at least two components, see Figs. 15b and c, to account for these asymmetry-structure features.

An even clearer structure in the left absorption line can be seen in the Mössbauer spectrum[55,64,65] of d-$Al_{65}Co_{15}Cu_{19.9}Fe_{0.1}$ which is shown in Fig. 16. There is a striking similarity of the shapes of P(Δ)'s in both alloys, compare Figs. 15c and 16c; the low-Δ P(Δ) is single-peaked, whereas the high-Δ has a bimodal character. Also the $\bar{\delta}$ and $\bar{\Delta}$ values are quite similar. This strongly suggests that the quasicrystalline structures must be very similar in both alloys.

It should be stressed here that, because of the so-called non-uniqueness problem, see Chapter 5 of this book, the P(Δ)'s derived here from the zero-field Mössbauer spectra of quasicrystals may not be unique. Within the boundary of the solution domain in the Mössbauer parameter space, other, slightly different P(Δ)'s also fit the spectra well.[55,65] The solution domain, and thus the possible P(Δ)'s, can be significantly narrowed by performing in-field Mössbauer spectroscopy. What seems to be certain, however, is the presence of two distinct classes of iron environments in many quasicrystalline systems.

There are several different structural models which attempt to describe the structure of d-Al-Co-Cu alloy.[12] One of them is the model suggested by Burkov.[68] Kramer et al.[50] calculated

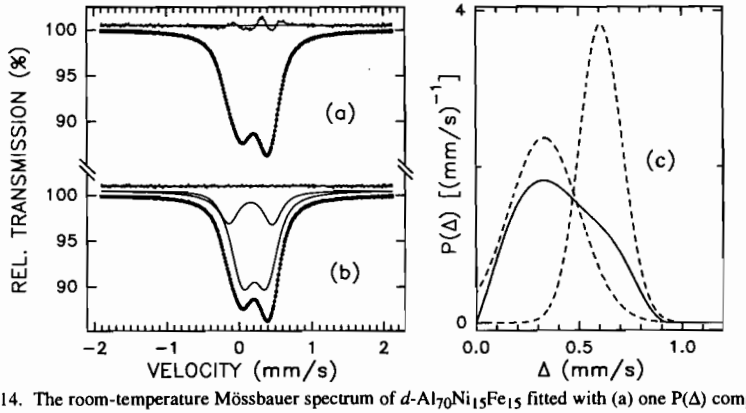

Figure 14. The room-temperature Mössbauer spectrum of d-$Al_{70}Ni_{15}Fe_{15}$ fitted with (a) one P(Δ) component, the solid line in (c), and (b) two P(Δ) components, the broken lines in (c). The P(Δ) component spectra are also shown in (b). The residuals, multiplied by a factor of three, are shown above each spectrum.

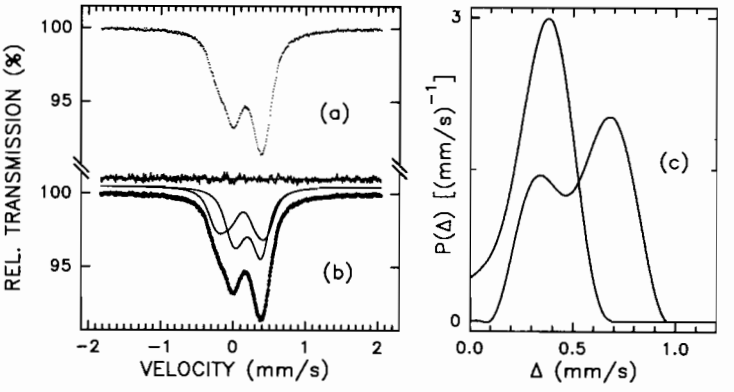

Figure 15. The room-temperature Mössbauer spectrum of d-$Al_{70}Co_{15}Ni_{14.9}Fe_{0.1}$, (a) the unfitted spectrum, (b) the spectrum fitted with two P(Δ) components, the solid lines in (c). The residuals, multiplied by a factor of three, are also shown in (b).

for this model, which corresponds to the composition $Al_{62}Co_{19}Cu_{19}$, the Mössbauer hyperfine parameters and the resulting Mössbauer spectrum. This theoretical spectrum is compared in Fig. 17 with the fit from Fig. 16b. It is clear from this comparison that theory and experiment do not agree. There are two major reasons for this, either the Burkov model[68] is incorrect or the calculations, due to their inherent limitations,[50] require some refinement. It should be noted that similar calculations carried out for c-$Al_{13}Fe_4$ resulted in a modest agreement between the predicted and measured Mössbauer spectra.[50] Recent calculations[69] for the composition $Al_{61.8}Co_{17.7}Cu_{20.5}$, which are based on a modified Burkov model in which copper atoms

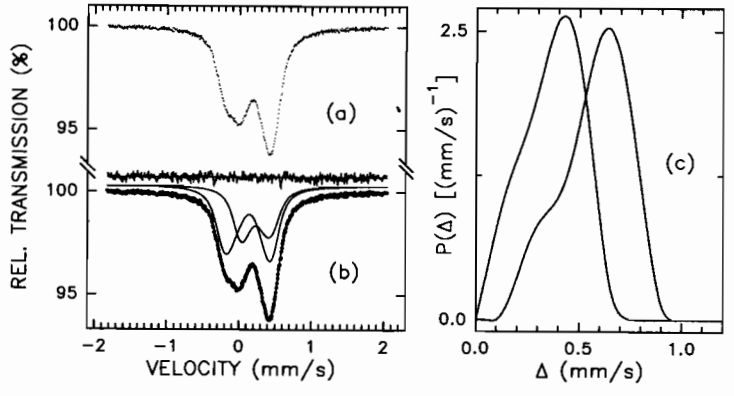

Figure 16. The room-temperature Mössbauer spectrum of d-$Al_{65}Co_{15}Cu_{19.9}Fe_{0.1}$. (a) the unfitted spectrum, (b) the spectrum fitted with two P(Δ) components, the solid lines in (c). The residuals, multiplied by a factor of three, are also shown in (b).

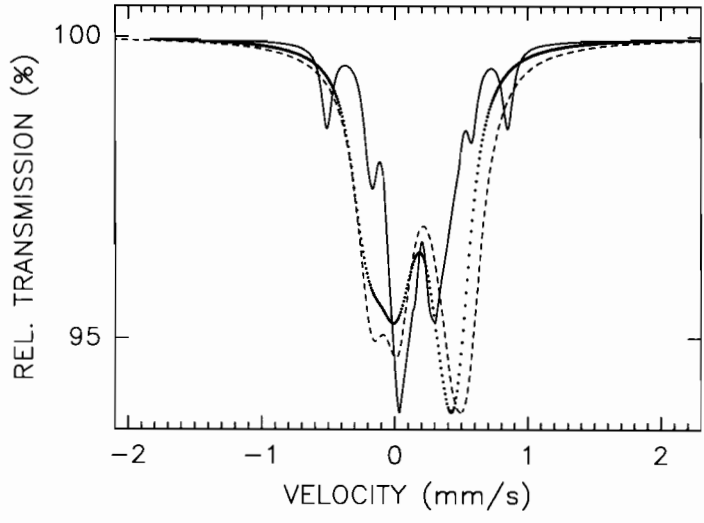

Figure 17. A comparison between the fit from Fig. 16(b), the dots, and the theoretical Mössbauer spectra calculated for the Burkov model,[50] the solid line, and for the modified Burkov model,[69] the broken line. The theoretical spectra were shifted horizontally so that their average isomer shift coincides with that of the fit.

occupy some of the cobalt positions, lead to a theoretical spectrum which is in a much better agreement with the experimental spectrum, see Fig. 17.

The experimental observation of two distinct P(Δ)'s, as shown in Figs. 15 and 16, implies the existence of two basic building blocks, or clusters, in the structure of the *d*-Al-Co-Ni and *d*-Al-Co-Cu alloys. This observation would thus favor structural models which are based on two such blocks. Recently, a new structural model of *d*-Al-Co-Cu has been proposed.[70] It assumes that there are two primary atom arrangements, or clusters, formed from an icosahedron by removing the atoms on two opposing vertices to form pentagonal polyhedra. The large pentagonal polyhedron cluster consists of ten aluminum atoms surrounding a cobalt or copper atom at the centre. The model does not differentiate between the cobalt and copper atoms whose atomic radii differ by only about two percent. In the smaller cluster, five cobalt or copper atoms replace the aluminum atoms in one pentagon, and an aluminum atom is located in the interior. These clusters are then properly connected to form aggregates, which in turn can be arranged to form a crystalline or quasicrystalline structure.[70] The geometry of these model clusters implies that one could expect qualitatively two different classes of transition metal sites, a conclusion that agrees with the experimental observation, see Fig. 16. Obviously, calculations of the Mössbauer hyperfine parameters for these two-cluster model are required to convincingly determine its compatibility with the Mössbauer results.

4. 1. 3. In-field Mössbauer Spectroscopy of Quasicrystals

Due to the nature of the 3/2 → 1/2 Mössbauer transition in iron-57, zero-field spectra discussed above provide only a distribution of the absolute values of

$$\Delta = 1/2\, eV_{zz}Q(1 + \eta^2/3)^{1/2}.$$

However, more stringent constraints can be imposed on possible theoretical models of the local atomic structure of quasicrystals if both the distributions of V_{zz} and η are known, as was successfully demonstrated for amorphous alloys.[71] In principle, such distributions can be extracted from in-field Mössbauer spectra.

A review[49] of in-field Mössbauer spectroscopy results for quasicrystals indicates that this method had a rather limited impact on elucidating structural properties of quasicrystals. This is because all studied quasicrystals, except for one case of *i*-$Al_{65}Cu_{20}Fe_{15}$, see reference 62, were metastable and thus possessed a significant amount of strain induced by the method of production; this resulted in a broadening or washing out of possible fine structural features in P(Δ). The stable *i*-Al-Cu-Fe alloys exhibit a single-peaked, Gaussian-like P(Δ), see Figs. 9b and d, and the moderate external magnetic fields applied[62] do not produce enough structure in the measured Mössbauer spectra. The main result of the in-field experiments[49] is the observation of a preponderance of the negative values of V_{zz} in *i*-alloys and of the positive values of V_{zz} in *d*-alloys. It is not clear, however, how this result relates to the atomic structure of the studied quasicrystals.

The in-field Mössbauer spectroscopy, with applied magnetic fields larger than about 7 T, has a potential for making a significant impact in structural studies of high-quality stable quasicrystals which exhibit a clear structure in their P(Δ)'s. The Mössbauer results, however, must be related to theoretical calculations of the electric field gradient tensor for various possible structural models. The latter is a challenging endeavour, but the first attempt has already been completed.[50,69]

4. 1. 4. Two Classes of Manganese Sites

The notion of two separate *classes* of manganese sites, not to be confused with the erroneous concept[49] of the two distinct manganese sites, in paramagnetic Al-Mn-based *i*-alloys, distinguished by the presence or absence of a localized magnetic moment, was suggested on the basis of various experimental results.[20,72] Perhaps the most convincing experimental proof came from the in-field Mössbauer measurements.[73,74] The magnetic susceptibility measurements[73,74] on the paramagnetic *i*-Al-Mn-Si alloys, in which a fraction of manganese atoms was substituted by iron atoms, showed that the effective magnetic moment per transition metal did not change with substitution. This is contrary to what is expected if all manganese atoms carry a magnetic moment. The in-field Mössbauer spectra showed, see Fig. 18, that the measured hyperfine magnetic field turned out to be the same as the applied magnetic field.[73,74] This is possible only for iron atoms with no local magnetic moment. Thus iron atoms substitute for only one class of manganese atoms - the class with zero magnetic moment.

The origin of these two classes of manganese sites seems to be related to the volume occupied by manganese atoms.[72,74] For large volumes manganese atoms carry no magnetic moment, whereas for small volumes manganese atoms possess a magnetic moment. Model electronic structure calculations carried out for an $Al_{80}Mn_{20}$ quasicrystal[75] support the concept of two classes of manganese sites. They predict the existence of manganese sites with a

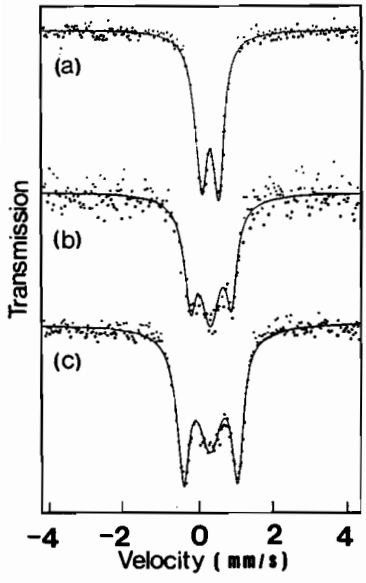

Figure 18. The Mössbauer spectra of i-$Al_{72}(Mn_{0.99}Fe_{0.01})_{22}Si_6$ measured at 4.2 K in external magnetic fields of (a) 0.0 T, (b) 3.0 T, and (c) 4.5 T. Figure obtained from reference 73.

quasigap in the density of states at the Fermi level and no magnetic moment, and of manganese sites with a peak in their density of states and a magnetic moment. As is discussed below, these two classes of magnetic sites are also present in magnetically ordered icosahedral alloys.

4. 2. *Magnetically Ordered Icosahedral Alloys*

The majority of known quasicrystals are not magnetically ordered. They exhibit paramagnetic, diamagnetic, or spin-glass properties.[20] There are reports[8] on the observation in metastable Al-Fe-Ce, Al-Mn-Si, Al-Ge-Mn, and Al-Ge-Cu-Mn icosahedral alloys of an unusual ferromagnetic behavior characterized by a very small value of magnetization and relatively high value of the Curie temperature. Unfortunately, the samples in these alloys cannot be produced in a single-phase form. Therefore, one has to carry out careful investigations with several techniques to separate the magnetic contributions from the possible magnetically-ordered second phases and from the icosahedral phase. As is shown below for the i-Al-Ge-Cu-Mn system, Mössbauer spectroscopy, combined with x-ray diffraction and magnetization measurements, proved very useful in separating magnetic contributions, which are intrinsic to the icosahedral phase, from those resulting from the impurities.

A thorough analysis of x-ray diffraction patterns[9,10] clearly indicates the presence in i-Al-Ge-Cu-Mn alloys of a ferromagnetic impurity, AlGeMn, whose Curie temperature of 519 K is very close to the values reported for these alloys.[9,10] Furthermore, the temperature dependence of the magnetization of the i-Al-Ge-Cu-Mn samples is very similar to that of the AlGeMn

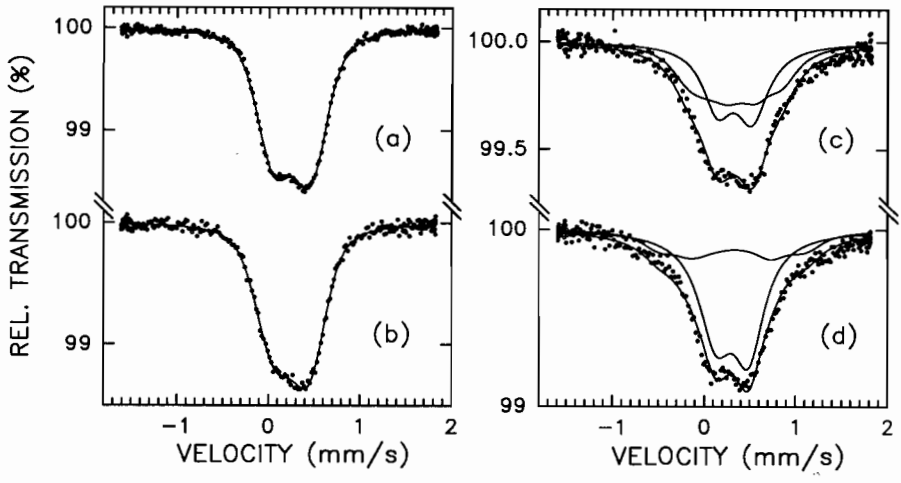

Figure 19. The Mössbauer spectra of i-$Al_{40}Ge_{25}Cu_{10-x}Fe_xMn_{25}$ obtained at room temperature for samples with x values of 0.06, (a), and 3, (b), fitted with one Gaussian P(Δ) component, the solid lines, and at 4.2 K for samples with x values of 0.06, (c), and 3, (d), fitted with the paramagnetic and magnetic components, as described in the text. Figure obtained from reference 76.

ferromagnet, except for a temperature region below about 30 K, where the magnetization suddenly increases nonlinearly.[10] In addition, the room-temperature Mössbauer spectra[9,10,76] of i-$Al_{40}Ge_{25}Cu_{10-x}Fe_xMn_{25}$ are clearly paramagnetic doublets, see Fig. 19a and b.

The 4.2 K Mössbauer spectra of i-$Al_{40}Ge_{25}Cu_{10-x}Fe_xMn_{25}$ cannot be fitted successfully with one magnetic component, as is explained in detail elsewhere.[9] A successful fit requires magnetic and nonmagnetic components,[9,76] see Figs. 19c and d. This means that there are also two classes of magnetic transition metal atoms in magnetically ordered icosahedral alloys and that iron atoms enter both of them. Furthermore, as is evidenced by the areas of the magnetic and nonmagnetic components, see Figs. 19c and d, iron atoms enter randomly both classes of transition metal sites for very small iron concentrations. However, for larger concentrations, iron atoms seem to enter preferentially the nonmagnetic class of transition metal sites.

It was concluded from the combination of the magnetization and the 4.2 K and room-temperature Mössbauer spectral studies[9,76] that the transition from a paramagnetic to a magnetic state, which is intrinsic to the i-Al-Ge-Cu-Mn system, must occur below 100 K. The temperature of this transition was determined from the analysis of the Mössbauer spectra measured at different temperatures.[10] An additional broadening of the spectra below 30 K is reflected in the divergence of the electric quadrupole interaction parameters,[10] as is shown in Fig. 20. It can be thus concluded that, in spite of the presence of the ferromagnetic AlGeMn impurity in the i-Al-Ge-Cu-Mn system, a careful analysis of Mössbauer spectra, combined with other experimental techniques,[9,10,76] made it possible to determine the intrinsic ordering temperature of about 30 K in this system and the value of iron magnetic moment of about 0.2 to 0.3 μ_B for the iron atoms entering the magnetic transition metal sites.

Recently, new magnetically-ordered, metastable, single-phase icosahedral alloys in the Al-B-Pd-Mn were discovered,[77] which are characterized by high values of ca. 500 K for their ordering temperatures[78] and of the magnetization, for example, 18.9 emu/g for i-$Al_{64}B_6Pd_{15}Mn_{15}$ at 4.2 K in a field of 2 T.[78] NMR studies[78] showed that the manganese atoms

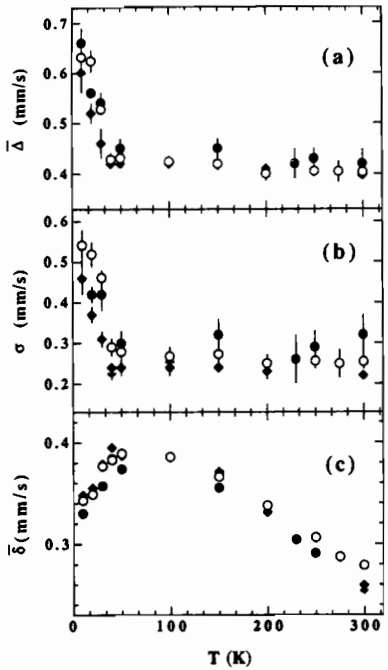

Figure 20. The temperature dependence of $\bar{\Delta}$ (a), the standard deviation σ of P(Δ) (b), and $\bar{\delta}$ (c) derived from fitting the Mössbauer spectra of i-$Al_{40}Ge_{25}Cu_{10-x}Fe_xMn_{25}$ [(♦) for x=0.1, (●) x=0.3, and (○) x=3, with one P(Δ) component. Figure obtained from reference 10.

with and without a magnetic moment coexist in these alloys. The Mössbauer spectra[79] of i-$Al_{64}B_6Pd_{15}Mn_{14.925}Fe_{0.075}$ at room-temperature and at 5.0 K, see Figs. 21a and b, show no evidence of ordering of the iron atoms. They can be fitted with two P(Δ)'s, as is shown in Fig. 21c. This confirms the NMR result[78] concerning the existence of the nonmagnetic class of

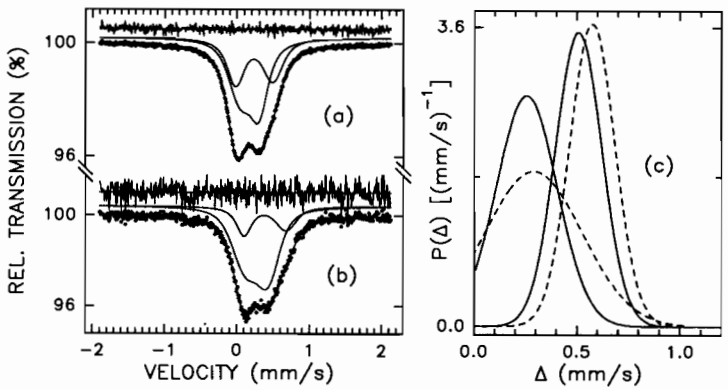

Figure 21. The Mössbauer spectra of i-$Al_{64}B_6Pd_{15}Mn_{14.925}Fe_{0.075}$ at room temperature (a) and at 5.0 K (b) fitted with two P(Δ), the solid and broken lines in (c), components also shown in (a) and (b). The residuals, multiplied by a factor of three, are shown above each spectrum.

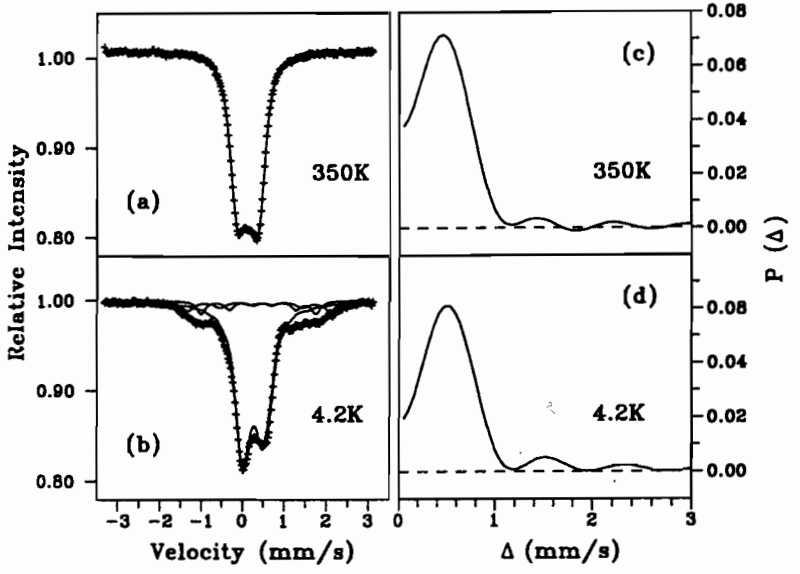

Figure 22. The Mössbauer spectra of i-$Al_{62.5}B_{7.5}Pd_{15}Fe_{15}$ measured at 350 K (a) fitted with one P(Δ), (c), and at 4.2 K (b) fitted with the P(Δ), (d), and the Zeeman components. The component spectra are indicated in (b). Figure obtained from reference 80.

manganese sites and indicates that there are two distinct environments around nonmagnetic Mn(Fe) atoms in this system.

It was recently discovered that completely replacing manganese atoms by iron atoms in the i-Al-B-Pd-Mn system retains both the icosahedral symmetry and the magnetism.[80] The Mössbauer spectra, shown in Fig. 22, of an icosahedral alloy of this system with an ordering temperature of 305 K provide unquestionable evidence for the existence of the magnetic and nonmagnetic classes of iron sites.

5. QUASICRYSTALS AND DISORDER

As mentioned in Section 1, before the discovery of stable quasicrystals, the available metastable samples contained significant amount of disorder and second phases which hindered the detection of properties which might be inherent to quasiperiodicity and led to significant confusion[8] in many areas of the physics of these alloys. Many stable quasicrystals are labelled "perfect," or "phason-free" because, from a diffraction point of view, their Bragg peaks are extremely sharp and their widths scale appropriately with the components of Q.[2-4,81] Yet, there is experimental evidence, which is summarized below, which indicates that these perfect quasicrystals contain some sort of disorder, which must then influence their physical properties.

The Mössbauer results reviewed above clearly indicate the presence of P(Δ) also in stable phason-free quasicrystals. Similar distributions are observed with other local probes, such as NMR and nuclear quadrupole resonance spectroscopy.[82] Such distributions of the hyperfine

parameters can only occur if there is a chemical and/or topological disorder in the investigated samples.

The diffuse scattering is often observed in x-ray and electron diffraction patterns of high-quality quasicrystals.[83] Such scattering indicates that some disorder is present in the diffracting structure. A recent study on the propagation of acoustic shear waves in a single-grain *i*-Al-Pd-Mn alloy shows the similarity of the acoustic properties of this alloy to those of amorphous metals.[84] The success of quantum interference theories,[3-6,14] which were originally developed for disordered conductors, in accounting for the temperature and field dependencies of the electrical conductivity and magnetoresistance of many stable quasicrystals also indicates the importance of disorder. The presence of disorder may also explain why the spikiness of the density of states predicted by theory, see Fig. 2, is not observed even in the ultra-high resolution ultraviolet photoemission spectroscopy valence bands, see Figs. 3 to 6. The presence of two magnetic classes of transition metal sites may also be related to disorder.[61]

There seem to be at least two qualitative reasons for the presence of disorder in high-quality stable quasicrystals. First, the concept of quasiperiodicity, by its very nature, stipulates that no two atoms in a quasilattice have exactly the same environment, which can be viewed as a sort of topological disorder. This must be in part responsible for the observed distribution of the hyperfine parameters studied with local probes. It may also cause the quasicrystals to become electronically disordered alloys, and hence, account for the success of the quantum interference theories. Second, there are at present about two dozen stable quasicrystals, see references 11, 12, and 22, all of which are ternary alloys. Clearly, one expects some chemical disorder to be present in such ternaries and such disorder is expected to lead to a smoothing out of the sharp characteristics of their physical properties, for example, of the spikiness in their density of states near the Fermi level, and/or their broadening, for example, compare the full width at half maximum of the $P(\Delta)$ for *i*-$Al_{64}Cu_{24}Fe_{12}$ with that for *i*-$Al_{65}Cu_{20}Fe_{7.5}Ru_{7.5}$, see Figs. 9d and 10c. Thus it seems that disorder has to be included in any attempts to explain the unusual physical properties of quasicrystals.

6. CONCLUDING REMARKS

Two major themes have been discussed in this chapter. The first theme is related to the electronic structure of quasicrystals because it is the knowledge and understanding of this structure which eventually will enable us to fully understand the unusual properties of these complex materials. The second theme is associated with the contribution of the recent Mössbauer spectral studies to elucidating some aspects of the structure and magnetism of quasicrystals.

Although the nature of the surprising transport properties is still unsolved, it seems that they may result from the combination of the low density of states at the Fermi level, localization effects, and the presence of the critical states. The quasiperiodicity by itself does not seem to be essential for the occurrence of these effects as they are also observed in structurally complex crystalline approximants.

After the first few years of confusion associated with poor quality samples and the problematic interpretation of their spectra, Mössbauer spectroscopy has emerged as an important experimental technique in studies of structural and magnetic properties of quasicrystals. It was instrumental, among other things, in establishing the occurrence of two classes of transition metal sites in many quasicrystals. It also provides, when used critically, reliable information on the quadrupole interaction distributions. However, this information by itself is not sufficient to answer the questions related to the structure of quasicrystals. It must

be compared with the theoretically predicted P(Δ)'s for possible structural models. Such a process is still in its infancy.

Magnetically ordered quasicrystals require in-field Mössbauer measurements to determine their type of ordering. Such measurements are also needed for diamagnetic and paramagnetic quasicrystals in order to impose further constraints on the derived hyperfine parameters from zero-field spectra, which is essential for using these parameters to discriminate between possible structural models. It is the belief of the author that Mössbauer spectroscopy is especially useful when used in combination with other experimental techniques, especially in the area of magnetism.

All Mössbauer spectral studies performed so far have been done with the iron-57 isotope. However, new quasicrystals with zinc and the rare-earth elements are now available. Mössbauer spectroscopy on other nuclei would undoubtedly provide valuable data on the local properties of these new quasicrystals.

ACKNOWLEDGEMENTS. This work was supported by the Natural Sciences and Engineering Research Council of Canada. The author is grateful to Professors A.-P. Tsai, A. Inoue, K. Edagawa, and S. Takeuchi for providing high-quality quasicrystalline samples and to Professor Y. Baer in whose laboratory the ultra-high-resolution photoemission experiments were carried out.

REFERENCES

1. D. Shechtman, I. Blech, D. Gratis, and J. W. Cahn, *Phys. Rev. Lett.* **53**, 1951 (1984).
2. A. I. Goldman and K. F. Kelton, *Rev. Mod. Phys.* **65**, 213 (1993); K. F. Kelton, *Int. Mat. Rev.* **38**, 105 (1993).
3. C. Janot, *Quasicrystals: A Primer*, Oxford University Press, Oxford (1992).
4. D. P. DiVincenzo and D. P. Steinhardt, eds., *Quasicrystals, The State of the Art*, World Scientific, Singapore (1991); A. I. Goldman and M. Widom, *Ann. Rev. Phys. Chem.* **42**, 685 (1991).
5. S. J. Poon, *Adv. Phys.* **41**, 303 (1992), and references therein.
6. Z. M. Stadnik and M. Akbari-Moghanjoughi, unpublished results.
7. Z. M. Stadnik, G. W. Zhang, M. Akbari-Moghanjoughi, A. P. Tsai, and A. Inoue, *Int. J. Mod. Phys.*, in press.
8. R. C. O'Handley, R. A. Dunlap, and M. E. McHenry, in *Handbook of Magnetic Materials*, K. H. J. Buschow, ed., Vol. 6, p. 453, Elsevier, Amsterdam (1991), and references therein.
9. Z. M. Stadnik and G. Stroink, *Phys. Rev. B* **43**, 894 (1991); **44**, 4255 (1991).
10. S. Nasu, M. Miglierini, and T. Kuwano, *Phys. Rev. B* **45**, 12778 (1992); M. Miglierini and S. Nasu, *J. Phys. Soc. Japan* **60**, 2135 (1991).
11. Z. M. Stadnik, G. W. Zhang, A. P. Tsai, and A. Inoue, *Phys. Rev. B* **51**, 4023 (1995), and references therein.
12. W. Steurer, *Mater. Sci. Forum* **150-151**, 15 (1994).
13. D. Mayou, C. Berger, F. Cyrot-Lackmann, T. Klein, and P. Lanco, *Phys. Rev. Lett.* **70**, 3915 (1993); F. S. Pierce, P. A. Bancel, B. D. Biggs, Q. Guo, and S. J. Poon, *Phys. Rev. B* **47**, 5670 (1993).
14. M. A. Chernikov, A. Bernasconi, C. Beeli, and H. R. Ott, *Europhys. Lett.* **21**, 767 (1993).
15. B. D. Biggs, S. J. Poon, and N. R. Munirathnam, *Phys. Rev. Lett.* **65**, 2700 (1990).
16. Y. Honda, K. Edagawa, A. Yoshioka, T. Hashimoto, and S. Takeuchi, *Japan J. Appl. Phys. A* **9**, 4929 (1994).

17. F. S. Pierce, S. J. Poon, and Q. Quo, *Science* **261**, 737 (1993); F. S. Pierce, Q. Quo, and S. J. Poon, *Phys. Rev. Lett.* **73**, 2220 (1994).
18. N. Mott, *Conduction in Non-Crystalline Materials*, Clarendon, Oxford (1993).
19. C. Berger, T. Grenet, P. Lindqvist, P. Lanco, J. C. Grieco, G. Fourcaudot, and F. Cyrot-Lackmann, *Solid State Commun.* **87**, 977 (1993).
20. S. Matsuo, T. Ishimasa, H. Nakano, and Y. Fukano, *J. Phys. F* **18**, L175 (1988); Z. M. Stadnik, G. Stroink, H. Ma, and G. Williams, *Phys. Rev. B* **39**, 9797 (1989), and references therein.
21. T. Klein, C. Berger, D. Mayou, and F. Cyrot-Lackmann, *Phys. Rev. Lett.* **66**, 2907 (1991); P. Lanco, T. Klein, C. Berger, F. Cyrot-Lackmann, G. Fourcaudot, and A. Sulpice, *Europhys. Lett.* **18**, 227 (1992); P. Lanco, C. Berger, F. Cyrot-Lackmann, and A. Sulpice, *J. Non-Cryst. Solids* **153-154**, 325 (1993).
22. Z. M. Stadnik, G. W. Zhang, A. P. Tsai, and A. Inoue, *Phys. Rev. B* **51**, 11358 (1995), and references therein.
23. P. A. Bancel and P. A. Heiney, *Phys. Rev. B* **33**, 7917 (1986); A. P. Tsai, A. Inoue, and T. Masumoto, *Mater. Trans., Japan Inst. Met.* **30**, 464 (1989); *ibid.* **30**, 666 (1989); A. Inoue, A. P. Tsai, and T. Masumoto, in *Quasicrystals*, T. Fujiwara and T. Ogawa, eds., p. 80, Springer-Verlag, Berlin (1990).
24. J. Friedel and F. Dénoyer, *C. R. Acad. Sci. Paris* **305**, 171 (1987); A. P. Smith and N. W. Ashcroft, *Phys. Rev. Lett.* **59**, 1365 (1987); V. G. Vaks, V. V. Kamyshenko, and G. D. Samolyuk, *Phys. Lett. A* **132**, 131 (1988); J. Friedel, *Helv. Phys. Acta* **61**, 538 (1988); *Philos. Mag. B* **65**, 1125 (1992).
25. K. Kimura, H. Iwahashi, T. Hashimoto, S. Takeuchi, U. Mizutani, S. Ohashi, and G. Itoh, *J. Phys. Soc. Japan* **58**, 2472 (1989); J. L. Wagner, B. D. Biggs, and S. J. Poon, *Phys. Rev. Lett.* **65**, 203 (1990).
26. F. Hippert, L. Kandel, Y. Calvayrac, and B. Dubois, *Phys. Rev. Lett.* **69**, 2086 (1992); E. A. Hill, T. C. Chang, Y. Wu, S. J. Poon, F. S. Pierce, and Z. M. Stadnik, *Phys. Rev. B* **49**, 8615 (1994).
27. S. E. Burko, T. Timusk, and N. W. Ashcroft, *J. Phys.: Condens. Matter* **4**, 9447 (1992); L. Degiorgi, M. A. Chernikov, C. Beeli, and H. R. Ott, *Solid State Commun.* **87**, 721 (1993); D. Macko and M. Kaspárková, *Philos. Mag. Lett.* **67**, 307 (1993); X. Wu, C. C. Homes, S. E. Burkov, T. Timusk, F. S. Pierce, S. J. Poon, S. L. Cooper, and M. A. Karlow, *J. Phys.: Condens. Matter* **5**, 5975 (1993).
28. M. A. Fradkin, *J. Phys.: Condens. Matter* **4**, 10497 (1992); A. E. Carlsson, *Phys. Rev. B* **47**, 2515 (1993).
29. M. Windisch, M. Krajcí, and J. Hafner, *J. Phys.: Condens. Matter* **6**, 6977 (1994), and references therein.
30. G. Trambly de Laissardière and T. Fujiwara, *Phys. Rev. B* **50**, 5999 (1994), and references therein.
31. M. Krajcí, M. Windisch, J. Hafner, G. Kresse, and M. Mihalkovic, *Phys. Rev. B* **51**, 17355 (1995).
32. Z. M. Stadnik, D. Purdie, M. Garnier, Y. Baer, A. P. Tsai, and A. Inoue, unpublished results.
33. Z. M. Stadnik, D. Purdie, M. Garnier, Y. Baer, K. Edagawa, and S. Takeuchi, unpublished results.
34. Z. M. Stadnik and G. Stroink, *Phys. Rev. B* **47**, 100 (1993).
35. M. Mori, S. Matsuo, T. Ishimasa, T. Matsuura, K. Kamiya, H. Inokuchi, and T. Matsukawa, *J. Phys.: Condens. Matter* **3**, 767 (1991).
36. M. Grioni, D. Malterre, and Y. Baer, *J. Low Temp. Phys.* **99**, 195 (1995).
37. U. Mizutani, Y. Sakabe, T. Shibuya, K. Kishi, K. Kimura, and S. Takeuchi, *J. Phys. Condens. Matter* **2**, 6169 (1990).
38. T. Takeuchi, Y. Yamada, U. Mizutani, Y. Honda, K. Edagawa, and S. Takeuchi, *Int. J. Mod. Phys.*, in press.
39. P. Lindqvist, C. Berger, T. Klein, P. Lanco, F. Cyrot-Lackmann, and Y. Calvayrac, *Phys. Rev. B* **48**, 630 (1993).
40. K. Wang, C. Scheidt, P. Garoche, and Y. Calvayrac, *J. Phys. (Paris)* **2**, 1553 (1992).

41. S. Takeuchi, *Mater. Sci. Forum* **150-151**, 35 (1994).
42. J. C. Phillips, *Phys. Rev. B* **47**, 7747 (1993); *ibid* **47**, 2522 (1993); *Solid State Commun.* **83**, 379 (1992); J. C. Phillips and K. M. Rabe, *Phys. Rev. Lett.* **66**, 923 (1991).
43. T. Klein and O. G. Symko, *Phys. Rev. Lett.* **73**, 2248 (1994).
44. K. Kimura and S. Takeuchi, in *Quasicrystals, The State of the Art* (Ref. 1), p. 313; K. Kimura, K. Kishi, T. Hashimoto, and S. Takeuchi, in *Quasicrystals*, K. H. Kuo and T. Ninomiya, eds., p. 233, World Scientific, Singapore (1991).
45. D. N. Basov, F. S. Pierce, P. Volkov, S. J. Poon, and T. Timusk, *Phys. Rev. Lett.* **73**, 1865 (1994).
46. H. Tsunetsugu, T. Fujiwara, K. Ueda, and T. Tokihiro, *J. Phys. Soc. Japan* **55**, 1420 (1986); *Phys. Rev. B* **43**, 8879 (1991); M. Kohmoto, B. Sutherland, and Ch. Tang, *ibid.* **35**, 1020 (1987); L. S. Levitov, *Europhys. Lett.* **7**, 343 (1988); K. Niizeki and T. Akamatsu, *J. Phys.: Condens. Matter* **2**, 2759 (1990); H. Tsunetsugu and K. Ueda, *Phys. Rev. B* **43**, 8892 (1991); B. Passaro, C. Sire, and V. G. Benza, *ibid.* **46**, 13751 (1992); C. Sire, B. Passaro, and V. Benza, *J. Non-Cryst. Solids* **153-154**, 420 (1993).
47. S. J. Poon, F. S. Pierce, and Q. Quo, *Phys. Rev. B* **51**, 2777 (1995).
48. N. P. Lalla, R. S. Tiwari, and O. N. Srivastava, *J. Phys.: Condens. Matter* **7**, 2409 (1995).
49. Z. M. Stadnik, *Hyp. Interact.* **90**, 215 (1994), and references therein.
50. P. Kramer, A. Quandt, M. Schlottmann, and T. Schneider, *Phys. Rev. B* **51**, 8815 (1995).
51. S. J. Campbell and F. Aubertin, in *Mössbauer Spectroscopy Applied to Inorganic Chemistry*, G. J. Long and F. Grandjean, eds., Vol. 3, p. 183, Plenum, New York, (1989); G. Le Caër and R. A. Brand, *Hyp. Interact.* **71**, 1507 (1992); R. E. Vandenberghe, E. De Grave, and P. M. A. de Bakker, *ibid.* **83**, 29 (1994).
52. D. G. Rancourt and J. Y. Ping, *Nucl. Instrum. Meth. Phys. Res. B* **58**, 85 (1991).
53. G. Le Caër and J. M. Dubois, *J. Phys. E* **12**, 1083 (1979).
54. J. Hesse and A. Rübartsch, *J. Phys. E* **7**, 526 (1974).
55. Z. M. Stadnik, A. P. Tsai, and A. Inoue, unpublished results.
56. Z. M. Stadnik, K. Edagawa, and S. Takeuchi, unpublished results.
57. A. Inoue, H. M. Kimura, T. Masumoto, A. P. Tsai, and Y. Bizen, *J. Mater. Sci. Lett.* **6**, 771 (1987); H. M. Kimura, A. Inoue, Y. Bizen, T. Masumoto, and H. S. Chen, *Mater. Sci. Eng.* **99**, 449 (1988).
58. C. L. Chien and K. M. Unruh, *Phys. Rev. B* **29**, 207 (1984); M. Maurer, J. M. Friedt, and J. P. Sanchez, *J. Phys. F* **15**, 1449 (1985); Z. M. Stadnik, F. Müller, G. Stroink, and M. Rosenberg, *J. Non-Cryst. Solids* **156-157**, 319 (1993).
59. S. Garçon, P. Sainfort, G. Regazzoni, and J. M. Dubois, *Scripta Met.* **21**, 1493 (1987); A. P. Tsai, A. Inoue, and T. Masumoto, *Japan J. Appl. Phys.* **26**, L1994 (1987).
60. N. Kataoka, A. P. Tsai, A. Inoue, T. Masumoto, and Y. Nakamura, *Japan J. Appl. Phys.* **27**, L1125 (1988); C. L. Chien and M. Lu, *Phys. Rev. B* **45**, 12793 (1992); M. Lu and C. L. Chien, *Hyp. Interact.* **71**, 1525 (1992).
61. R. A. Brand, G. Le Caër, and J. M. Dubois, *J. Phys.: Condens. Matter* **2**, 6413 (1990); *Hyp. Interact.* **55**, 903 (1990); Z. M. Stadnik, G. Stroink, G. Lamarche, and A. Inoue, *J. Phys. Soc. Japan* **60**, 3829 (1991); Z. M. Stadnik and F. Müller, *Philos. Mag. B* **71**, 221 (1995).
62. J. Teillet and B. Bouchet-Fabre, *Hyp. Interact.* **55**, 1077 (1990).
63. A. P. Tsai, A. Inoue, and T. Masumoto, *Mater. Trans., Japan Inst. Met.* **34**, 155 (1993).
64. M. Eibschütz, M. E. Lines, H. S. Chen, and F. A. Thiel, *Phys. Rev. B* **46**, 491 (1992).
65. Z. M. Stadnik, A. P. Tsai, and A. Inoue, in *Aperiodic '94, Proc. Int. Conf. Aperiodic Crystals*, G. Chapuis and W. Paciorek, eds., p. 259, World Scientific, Singapore (1995).
66. A. P. Tsai, A. Inoue, and T. Masumoto, *Philos. Mag. Lett.* **64**, 163 (1991); A. P.

Tsai, T. Masumoto, and A. Yamamoto, *ibid.* **66**, 203 (1992).
67. A. P. Tsai, A. Inoue, and T. Masumoto, *Mater. Trans., Japan Inst. Met.* **30**, 150 (1989); A. P. Tsai, N. Kataoka, A. Inoue, and T. Masumoto, *Japan J. Appl. Phys.* **29**, L1696 (1990).
68. S. E. Burkov, *Phys. Rev. B* **67**, 12325 (1993).
69. H. Teuscher, private communication.
70. S. G. Song and E. R. Ryba, *Philos. Mag. B* **69**, 707 (1994).
71. M. Maurer and J. M. Friedt, *Hyp. Interact.* **27**, 135 (1986), and references therein.
72. M. Eibschütz, M. E. Lines, H. S. Chien, and J. V. Waszczak, *Phys. Rev. B* **38**, 10038 (1988); M. Eibschütz, M. E. Lines, H. S. Chien, J. V. Waszczak, G. P Espinosa, and A. S. Cooper, *ibid.* **41**, 4606 (1990).
73. K. Edagawa, H. Ino, S. Nasu, K. Kimura, S. Takeuchi, T. Shinjo, K. Koga, T. Shimizu, and H. Yasuoka, *J. Phys. Soc. Japan* **56**, 2629 (1987); H. Ino, K. Edagawa, K. Kimura, S. Takeuchi, and S. Nasu, *Mater. Sci. Forum* **22-24**, 437 (1987).
74. M. Eibschütz, M. E. Lines, H. S. Chien, J. V. Waszczak, G. Papaefthymiou, and R. B. Frankel, *Phys. Rev. Lett.* **59**, 2443 (1987); *J. Appl. Phys.* **63**, 4063 (1988).
75. A. E. Carlsson, *Int. J. Mod. Phys. B* **7**, 293 (1993).
76. Z. M. Stadnik and G. Stroink, *Hyp. Interact.* **69**, 643 (1991).
77. Y. Yokoyama, A. Inoue, and T. Masumoto, *Mater. Trans., Japan Inst. Met.* **33**, 1012 (1992); *Mater. Sci. Eng. A* **181-182**, 734 (1994).
78. T. Shinohara, Y. Yokoyama, M. Sato, A. Inoue, and T. Masumoto, *J. Phys. Condens. Matter* **5**, 3673 (1993); *Mater. Sci. Eng. A* **181-182**, 798 (1994).
79. Z. M. Stadnik, G. W. Zhang, Y. Yokoyama, and A. Inoue, unpublished results.
80. C. R. Lin, C. M. Lin, S. T. Lin, and I. S. Lyubutin, *Phys. Lett. A* **196**, 365 (1995).
81. C. A. Guryan, A. I. Goldman, P. W. Stephens, K. Hiraga, A. P. Tsai, A. Inoue, and T. Masumoto, *Phys. Rev. Lett.* **62**, 2409 (1989); A. P. Tsai, H. S. Chen, A. Inoue, and T. Masumoto, *Phys. Rev. B* **43**, 8782 (1991).
82. A. Shastri, F. Borsa, D. R. Torgeson, and A. I. Goldman, *Phys. Rev. B* **50**, 4224 (1994); A. Shastri, F. Borsa, D. R. Torgeson, J. E. Shield, and A. I. Goldman, *ibid.* **50**, 15651 (1994).
83. K. Hradil, T. Proffen, F. Frey, K. Eichhorn, and S. Kek, *Philos. Mag. Lett.* **71**, 199 (1995); L. E. Levine and J. L. Libbert, *ibid.* **71**, 213 (1995).
84. N. Vernier, G. Bellessa, B. Perrin, A. Zarembovitch, and M. De Boissieu, *Europhys. Lett.* **22**, 187 (1993).